Modeling of Battery Life I.
The Equivalent Circuit Model (ECM) Approach

Bor Yann Liaw, Rudolph G. Jungst, Angel Urbina, and Thomas L. Paez
Sandia National Laboratories, Albuquerque, NM [1]

Accurately predicting a battery's life is an important issue for the energy storage community. It is also a long-standing challenge due to the tremendous technical difficulties that must be overcome to allow effective and reasonable prediction. Recently, with advancements in experimental techniques, numerical modeling, and computer simulation capabilities, we found that there exists an opportunity for us to address this issue by developing a sensible, concurrent approach using several types of numerical models to predict battery life via simulation. In this paper, we discuss how the equivalent-circuit model can be used in simulating battery performance, particularly the capacity change with cycling and aging conditions, to predict its cycle and calendar life. We are proceeding with experimental validation to corroborate our prediction from the models and enhance confidence in reaching a reliable estimate of battery life.

Introduction

Valve-regulated lead-acid (VRLA) batteries continue to be the most favorable system used in stationary energy storage applications due to its availability, maturity, and lower cost. Development of a battery life prediction capability is being pursued in this work, particularly for float type applications. The lack of such a prediction capability contributes to a general uncertainty regarding the need for battery replacement and forces one to replace cells prior to complete wear out in order to avoid system outages. The inability to predict battery failure has led to a situation in back up power applications where costly inspections and performance monitoring must be performed frequently to verify system readiness in case a utility power outage occurs. This situation is especially troublesome given that one of the expected benefits of a VRLA system is reduced maintenance cost. Inductive battery models forming an adaptive approach that can be used to anticipate failures seem to offer a favorable solution to this situation. The objective of this work is to predict battery failures accurately so that maintenance and replacements are furnished in a timely manner.

The approach we are taking consists of using (1) an equivalent circuit model (ECM) technique to simulate battery performance characteristics and augment the test data base, (2) a fuzzy logic (FL) technique to recognize degradation patterns and failure modes in the battery behavior, and (3) an artificial neural network (ANN) technique to train a model to predict battery life in an adaptive manner. Complicated impacts on the battery performance from the environmental and operating conditions can be effectively considered in the model to improve the capability and accuracy of prediction. This paper will focus on discussion of the ECM approach and how it can be used to simulate and predict battery performance and life.

The Equivalent Circuit Model (ECM)

We found that the ECM approach can be very simple but effective in modeling battery performance [1-4]. The ECM is primarily based on the cell's impedance response to external conditions imposed by a battery's operating regime. For energy storage applications, the operating regime usually includes two parts: the standby/storage mode and the mission/duty mode; each exhibits its unique impacts on the battery life. Our model must accommodate both modes in order to accurately predict battery life in an application. We will discuss how the model is constructed, battery performance simulated, and capacity fade predicted. The results of the ECM simulation will then be

[1] bliaw@hawaii.edu.
Sandia National Laboratories is a multi-program laboratory operated by Sandia Corporation, a Lockheed-Martin Company, for the United States Department of Energy's National Nuclear Security Administration under Contract DE-AC04-94AL85000. The USDOE FreedomCAR and Vehicle Technology Office through the ATD High-Power Battery Program funded the lithium-ion battery testing and data collection. Ford Motor Co. and US Department of Transportation provided partial funding for the VRLA battery testing and data collection. The battery life prediction modeling work was funded by USDOE under the Energy Storage Systems Program.

combined with experimental test data for the FL and ANN model developments for degradation and failure detection and adaptive battery life prediction, respectively.

Before we discuss the model construction, an important point worth making is that, in any battery modeling and simulation work, accurately predicting battery performance or life and thus achieving a high fidelity of simulation, relies on the availability of a set of data that adequately represents the battery chemistry. However, a useful amount of data for VRLA batteries is unavailable to us now. Therefore, we are using a set of data from a lithium-ion battery chemistry that was tested under the US Department of Energy Advanced Technology Development Program. Accelerated life testing [5,6] illustrates the validity of predicting calendar life under typical storage aging conditions, and another set of data collected for a nominal VRLA battery tested in our laboratory [7] for cycle life study under overcharging conditions demonstrates the viability of cycle life prediction.

Figure 1 illustrates the ECM used in this work. There are three major parts in the model. The first one is the static part shown on the upper left hand side of the diagram, representing battery's characteristic thermodynamic properties, such as the open circuit voltage (OCV) versus the state-of-charge (SOC) and the nominal capacity. V_o represents the cell voltage at a specific SOC as an initial condition. The second part is the combination of [R_1 + (R_2C)] shown on the upper right hand side of the diagram. The serial resistance R_1 represents the ohmic behavior of the cell, and the (R_2C) circuit the faradic. This is the dynamic response depicting the kinetic properties of the cell in reaction to any charge or discharge regime. The last part shown in the lower part of the diagram is either an electrical load for discharge or a source for charging, depending on the testing/operating conditions.

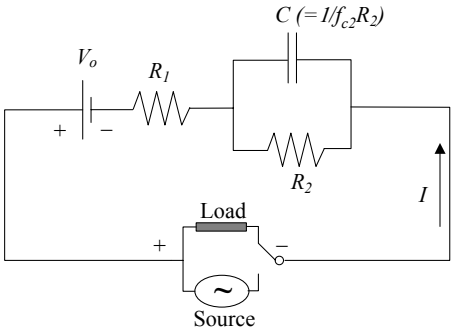

Figure 1. ECM used in this work.

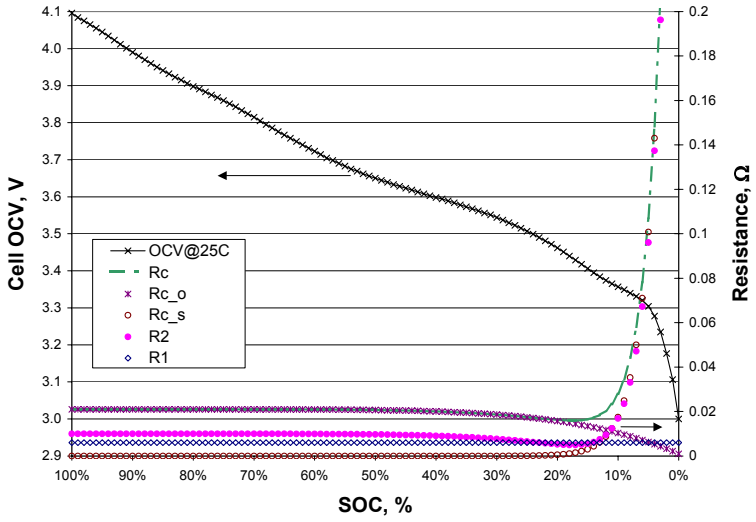

Figure 2. The OCV and resistance versus SOC curves needed for constructing a viable ECM for the specific battery.

To construct a valid ECM, we need to have the SOC-dependent OCV and resistance (R_1 and R_2) values incorporated into the model. In Figure 2, we show a set of SOC-dependent values for the lithium-ion battery cell chemistry used in this work to illustrate calendar life prediction. This particular chemistry was tested in a nominal 18650-sized lithium-ion cell consisting of MAG-10 graphite as the active negative electrode material, $LiNi_{0.8}Co_{0.15}Al_{0.05}O_2$ the active positive electrode material with poly(vinylidine difluoride) binder, and 1.2M $LiPF_6$ in ethyl carbonate/ethyl methyl carbonate (3:7 weight % ratio) electrolyte [5,6]. The OCV values were determined from a typical cell discharged at C/25 rate. The resistance versus SOC relationship can be derived from two sources of data: either from AC impedance measurements or from DC galvanostatic polarization, which yields discharge curves at different rates. A more detailed discussion of how to derive these values can be found in [8]. We should note that in the model, the total impedance R_c was assumed to consist of two independent components, R_c^o and R_c^s, as shown in Figure 2, to approximate the resistance change with SOC. The function of R_c^o follows a power law with SOC, while that of R_c^s is an exponential function with SOC. Although these functions are empirical and do not necessarily imply any physical meaning, the shape of the formula could provide us some clues as to what process might determine the physical change of the cell performance. The values of R_2 were obtained from subtracting R_1 from R_c. The capacitance, C, value can be derived from the characteristic frequency, $f_{c2} = 1/R_2C$, which is yielded from the

Nyquist plot of the cell as demonstrated in [8]. The time-dependent cell voltage can then be calculated from the ECM for a constant-current condition [4], according to (1):

$$V(t) = \frac{Q(0)}{C} e^{-t/R_2C} + V_o - IR_1 - IR_2\left(1 - e^{-t/R_2C}\right), \text{ (where } I = \text{constant)} \quad (1)$$

where $Q(0)$ is the nominal capacity, and V_o the nominal SOC-dependent cell OCV. Thus, for any given time step, the charge passed is calculated to derive the SOC value at the end of the step, and the associated OCV and resistance values are plugged into (1) to give the cell voltage as a function of time.

Similarly, for the VRLA model construction, we took a similar approach, where the SOC-dependent OCV and resistance values are shown in Figure 3.

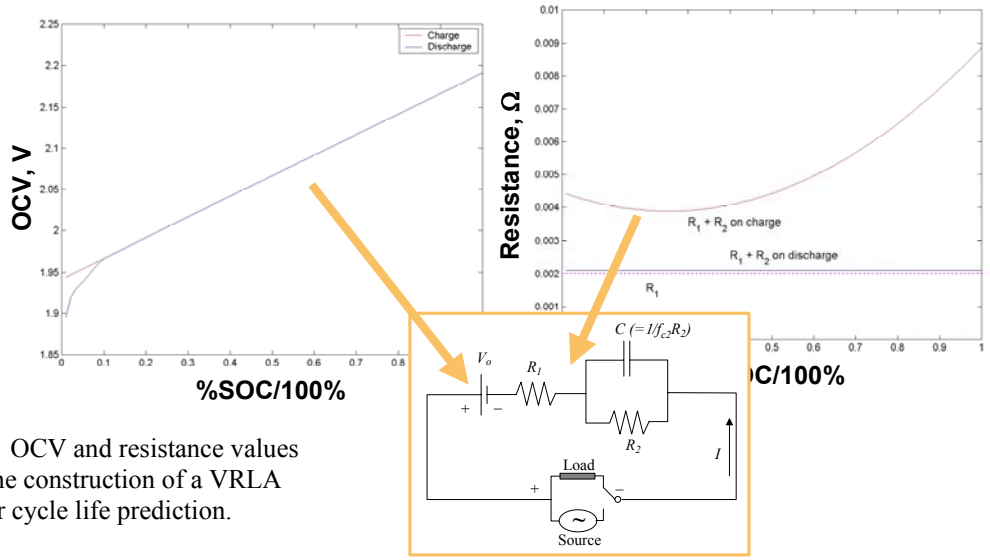

Figure 3. OCV and resistance values used in the construction of a VRLA model for cycle life prediction.

Results and Discussion

Figure 4 shows the simulated discharge curves of the nominal 18650-sized lithium-ion cell using the parameters depicted in Figure 2. The C/25 and C/1 rate curves were validated with experimental data reported in [5,6,8], and an excellent agreement was found, indicating a high fidelity of simulation has been obtained. A similar simulation and validation for the nominal VRLA cell [1] using the parameters shown in Figure 3 was also demonstrated as shown in Figure 5, where simulated C/3 rate charging and discharging curves are compared with the experimental data.

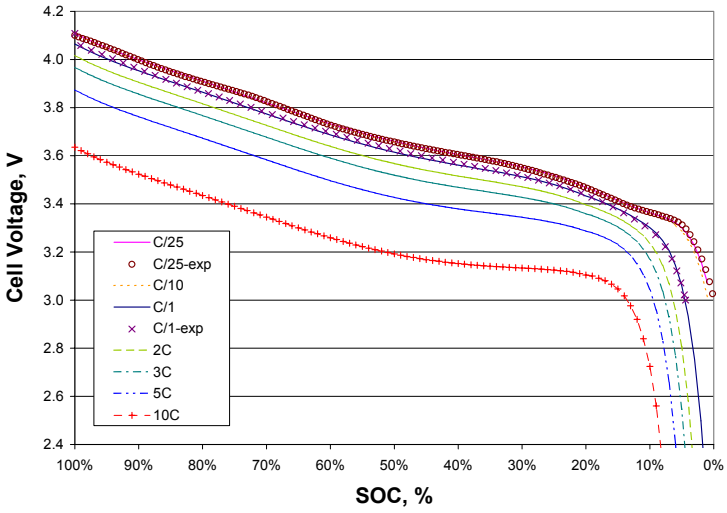

Figure 4. Discharge curves simulated for various rates in comparison with test data at C/25 and C/1 rates.

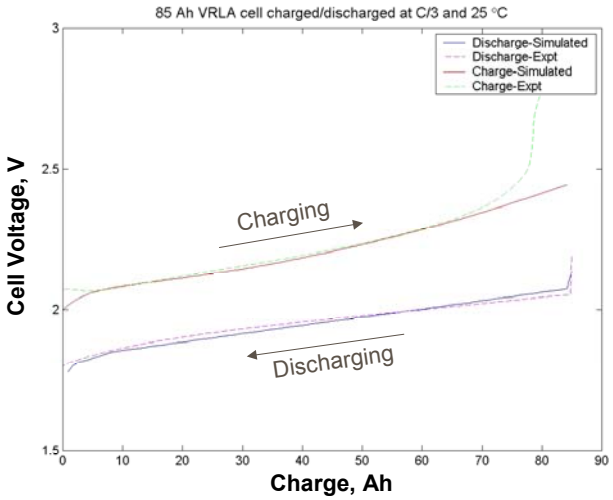

Figure 5. Simulated charging and discharging curves for a nominal VRLA cell at C/3 rate and compared with experimental results.

use the ECM to simulate the battery performance [1], reflecting the effect of mission or duty cycle on the battery life.

Figure 6 shows a series of thermal aging tests on a lithium-ion cell aged at 55°C and 100% SOC over about 20 weeks [5,6]. Every 4 weeks, the cell was taken out of aging and subjected to a reference performance test (RPT) [9], in which the C/1 capacity was determined, as shown in Figure 6. We observed increasing polarization resistance in the cell, which results in decreasing cell capacity. This behavior is better shown in Figure 7, where the polarization resistance of the cell is displayed as a function of SOC for each RPT after each subsequent 4 weeks of aging.

It is important to recognize that the cell resistance behavior as a function of SOC essentially has two distinct contributions; each also varies with SOC. This behavior is better recognized in the right-hand graph in Figure 7, where the two distinct contributions of resistance are shown as a function of SOC for RPT 5. The first contribution, which is dominant in the high SOC regime (>50% SOC), follows a power law. The second contribution, which dominates in the low SOC regime (<50% SOC), follows an exponential relationship with SOC. Equation (2) expresses the generic form of these two contributions:

$$R_2 = a + b\,(\mathrm{SOC})^c + d\,\exp((1\text{-SOC})\cdot e) \qquad (2)$$

It is also critical to realize that the second contribution of resistance determined the capacity of the cell under test and is thus the major factor that results in the capacity fade. It is not clear what the underlying mechanism is that caused this polarization resistance to rise and lead to capacity fade. Nonetheless, by assuming a consistent pattern of relationship for both contributions to the resistance increase with aging duration (Table 1), we were able to simulate

Built upon the confidence yielded from such validation, we can further explore the possibility of predicting the capacity for the cell under thermal aging or cycling conditions. The thermal aging approach is often used for accelerated life tests, and analysis and extrapolation of the accelerated life test results can lead to battery life prediction at operating conditions [5,6]. The thermal aging process provides us two aspects of information regarding degradation of the cell. One is how temperature accelerates the cell degradation, which can teach us how to model the temperature dependence of thermal degradation in the ECM. Another important aspect is the aging speed, which depicts the scale of how fast the degradation rate is and how it impacts the battery life. The aging phenomena directly affect the battery service life during the standby or storage mode. On the other hand, stressful cycling conditions can be imposed on cells for accelerated cycling life tests. In this case, we will show how a severe overcharging cycling can affect a VRLA cell cycle life [7] and how to

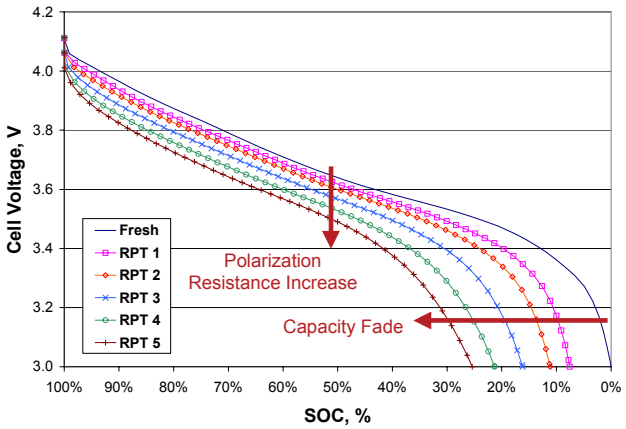

Figure 6. Discharging behavior of the lithium-ion cell after five sequential thermal aging tests, each lasting for 4 weeks, at 55°C and 100% SOC.

Table 1. Parameters used in equation (2): $R_2 = a + b\,(\mathrm{SOC})^c + d\,\exp((1\text{-SOC})\cdot e)$ for resistance calculation.

RPT	1	2	3	4	5
a	0.0099	0.0187	0.0488	0.0628	0.0745
b	0.03	0.04	0.05	0.06	0.08
c	1.7	1.5	1.3	0.5	0.5
d	4×10^{-6}	8×10^{-6}	1.6×10^{-5}	3.2×10^{-5}	6.4×10^{-5}
e	11.9	11.9	12	12	11.8

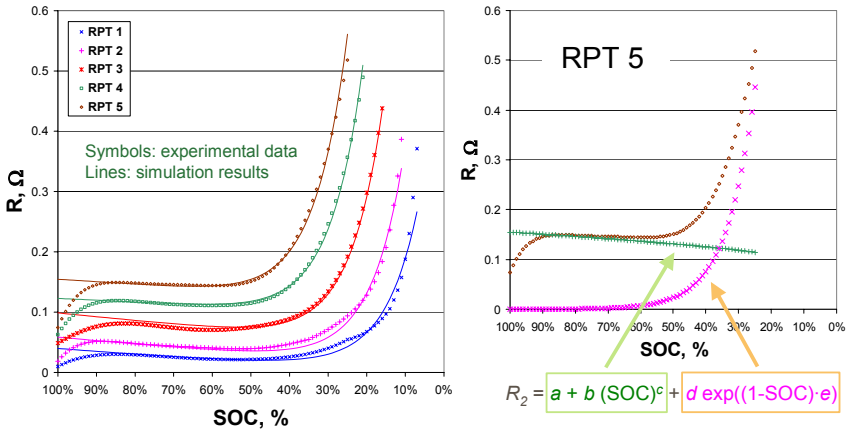

Figure 7. Polarization resistance changes as a function of SOC in the lithium-ion cell after five sequential thermal aging periods at 55°C and 100% SOC; each lasts for 4 weeks.

discharging curves for the five aging tests, as shown in Figure 8. The resulting capacity from the simulation is quite consistent with the experimental value determined from each RPT. This consistency indicates that our ECM prediction of the battery capacity fade is achievable. By examining the data for all aging conditions, we will be able to develop a correspondence between aging conditions and capacity fade for this chemistry. Thus the fading and calendar life of the cell can then be predicted.

Likewise, we can also assume that cell degradation from cycling conditions is reflected in the cell impedance changes. Figure 9 uses an example observed in a VRLA cell [7] that underwent a 40% overcharging and 100% discharge regime. The severe cycling regime was designed to accelerate the degradation from cycling so the cell's cycle life could be measured quickly. More detailed descriptions of the experimental setup and test protocols for this particular VRLA cell test were reported elsewhere [7,10] and will not be repeated here. The most important aspect found in the experiments was that at least two degradation mechanisms were associated with capacity fade, which in turn resulted in the failure of the cell operation. In the

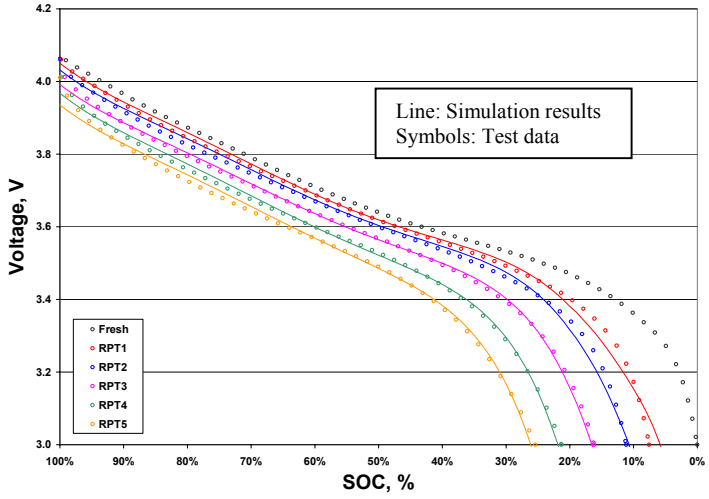

Figure 8. Simulated discharging curves based on a set of parameters that follow a consistent relationship with aging duration as listed in Table 1.

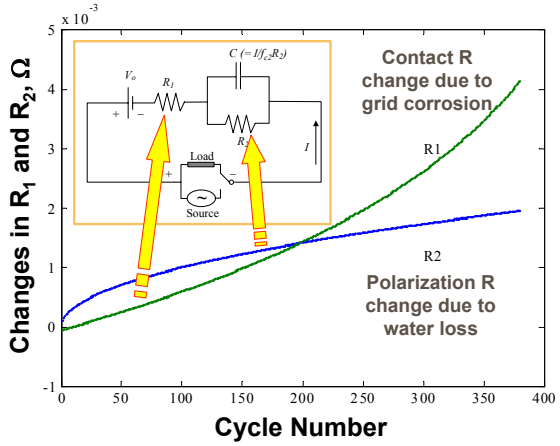

Figure 9. Resistance change with cycle number in the VRLA test cell due to different degradation mechanisms.

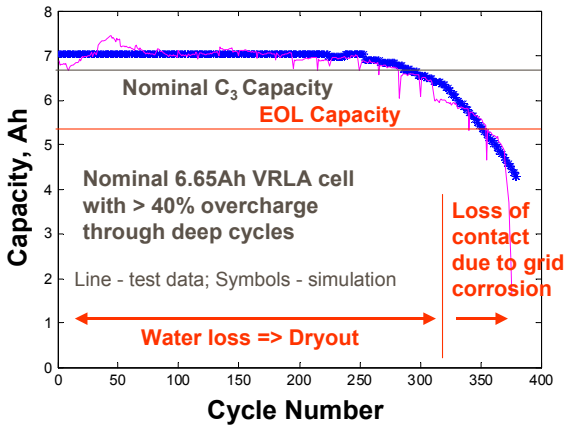

Figure 10. Cell capacity change with cycle number as simulated from the ECM using parameters shown in Figure 9.

initial stage, the overcharging caused cell gassing and venting, which subsequently led to water loss and cell imbalance. This was the cause for the capacity fade that appeared around 250 cycles as a result of repeated continuous overcharging and deep discharging tests. The second degradation process became dominant after the cell suffered from the results of repeated severe gassing, which causes a significant expansion in the electrode active materials and a gradual loss of contact with the grid. Repeated overcharging also caused severe grid corrosion, particularly in the positive plates. The combination of electrode expansion and grid corrosion led to increased contact resistance, as shown in Figure 9, and eventually the cell's failure. The transition in the cell capacity fade rate around 320 cycles revealed the change in the degradation mechanism that led to failure.

Using the resistance values shown in Figure 9, in which the contact resistance change was included in R_1 and the faradic polarization resistance increase associated with water loss in R_2, we were able to calculate the resulting capacity for each cycle under the repeated overcharging and discharge regime. The capacity as a function of cycle number is shown in Figure 10, where experimental data and the simulated results are compared. As the resistance values changed with cycle number, the resulting capacity fade was also varied. The simulation captured the resulting capacity fade rate change via the incorporation of the mechanism change. We therefore successfully modeled the cell degradation and cycle life for this nominal VRLA cell.

Conclusion

A simple ECM was used in this work to show that, with a sufficient amount of data collected and a sufficient understanding of the battery degradation process, we can develop a highly reliable battery performance model to predict either calendar or cycle life. Thermal aging is the most common cause of cell degradation related to calendar life. Repeated overcharging and deep discharging are frequently the major causes of cell degradation in cycle life. Our simulation captured both important aspects of the degradation processes in the calendar and cycle life behavior. Thus life prediction can be achieved and validated for both standby/storage and mission/duty periods. When available, this subset of data can then be used in the ANN model development for adaptive battery life prediction.

References

1. B. Y. Liaw, presented in the Joint Meeting of International Battery Association and the 5th Hawaii Battery Conference 2003, Waikoloa, Hawaii, January 7-10, 2003.
2. E. Barsoukov, J. H. Kim, C. O. Yoon, and H. Lee, *J. Power Sources*, **83**, 61 (1999).
3. E. Karden, S. Buller, and R. W. De Doncker, *Electrochimica Acta*, **47**, 2347 (2002).
4. M. W. Verbrugge and R. S. Conell, *J. Electrochem. Soc*., **149**, A45 (2002).
5. R. G. Jungst, D. H. Doughty, B. Y. Liaw, G. Nagasubramanian, H. L. Case, and E. V. Thomas, in *Proceedings of the 40th Power Sources Conference*, Cherry Hill, NJ, June 2002.
6. R. G. Jungst, G. Nagasubramanian, H. L. Case, B. Y. Liaw, A. Urbina, T. L. Paez, D. H. Doughty, *J. Power Sources*, **119-121**, 870 (2003).
7. K. P. Bethune and B. Y. Liaw, presented in the 201st Electrochemical Society Meetings, Philadelphia, PA, May 12-17, 2002.
8. B. Y. Liaw, G. Nagasubramanian, R. G. Jungst, D. H. Doughty, presented in the 14th International Conference on Solid State Ionics, June 22-27, 2003, Monterey, CA; to be published in *Solid State Ionics*.
9. *PNGV Test Plan for Advanced Technology Development Gen 2 Lithium-Ion Cells*, EHV-TP-121, Revisions 1 through 6, USDOE.
10. K. P. Bethune and B. Y. Liaw, to be published in *J. Power Sources*.